University of Zawia Journal of Engineering Sciences and Technology (UZJEST)
Volume 4, Issue 2, (2026), pp 75-95, ISSN 3006-2764

Local Polynomial Operator Interpolation for Tunable Rational Dynamical Models

Fathi Bribesh[*1], Hamza Daoub[2]

[1] Department of Mathematics, Faculty of Sciences, University of Zawia, Zawia, Libya.

[2] Department of Mathematics, School of Basic Science, The Libyan Academy of Postgraduate Study, Tripoli, Libya.

*Corresponding author email: f.bribesh@zu.edu.ly

Received: 22-06-2026 | Accepted: 29-08-2026 | Available online: 09-09-2026 | DOI:10.26629/uzjest.2026.07

ABSTRACT

This paper introduces a local polynomial operator interpolation framework for constructing tunable rational dynamical models between selected integer-order regimes. For a fixed interpolation degree k, the operator $D_\alpha^{(k)}$ is defined as a finite linear combination of classical integer-order derivatives with Lagrange coefficients depending on a real parameter α. The construction recovers the classical derivatives at the interpolation nodes, remains finite-dimensional, and satisfies basic stability estimates on fixed stencils. Since its Laplace symbol $\sigma_\alpha^{(k)}(s)$ is a polynomial in s, equations involving $D_\alpha^{(k)}$ reduce to finite-order ordinary differential equations and yield rational transfer functions. The proposed operator is a local rational alternative for applications where tunability, interpretability, and computational simplicity are more important than long-memory modelling.

Keywords: Interpolatory operators, polynomial operator interpolation, integer-order models, control-oriented modelling.

الاستيفاء المحلي للمؤثرات متعددة الحدود في النماذج الديناميكية النسبية القابلة للضبط

فتحي بريبش[1]، حمزة داعوب[2]

[1] قسم الرياضيات، كلية العلوم، جامعة الزاوية، الزاوية، ليبيا

[2] قسم الرياضيات، مدرسة العلوم الأساسية، الاكاديمية الليبية للدراسات العليا، طرابلس، ليبيا

ملخـــــص البحـــــث

يُقدِّم هذا البحث إطار استيفاء عامل تفاضلي متعدد الحدود محليّاً لبناء نماذج ديناميكية نسبية قابلة للضبط بين أنظمة الرتبة الصحيحة المُختارة. بالنسبة لدرجة استيفاء ثابتة $\mathbf{k}$، يُعرَّف المؤثر $\mathbf{D_\alpha^{(k)}}$ كتركيبة خطية منتهية من المشتقات التقليدية ذات الرتبة الصحيحة، مع معاملات لاجرانج تعتمد على وسيط حقيقي $\boldsymbol{\alpha}$. يستعيد هذا البناء المشتقات التقليدية عند عقد الاستيفاء، ويظل محدود الأبعاد، ويحقق تقديرات استقرار أساسية على قوالب ثابتة. وبما أن رمز لابلاس الخاص به $\boldsymbol{\sigma_\alpha^{(k)}(s)}$ هو متعددة حدود في $\mathbf{s}$، فإن المعادلات التي تشمل $\mathbf{D_\alpha^{(k)}}$ تختزل إلى معادلات تفاضلية عادية محدودة الرتبة، وتُنتج دوال نقل نسبية. يُشكِّل المؤثر المُقترَح بديلاً نسبياً محلياً للتطبيقات التي تكون فيها قابلية الضبط، وقابلية التفسير، والبساطة الحسابية أكثر أهمية من نمذجة الذاكرة الطويلة.

الكلمات الدالة: مؤثرات استيفائية، استيفاء المؤثر متعدد الحدود، نماذج الرتبة الصحيحة، النمذجة الموجهة للتحكم.

1. Introduction

Integer-order differential equations are the standard foundation for modelling dynamical systems in applied mathematics, engineering, and control. Their main advantages are well known as they are local, finite-dimensional in many practical settings, and compatible with classical tools from ordinary differential equations, functional analysis, Sobolev spaces, semigroup theory, and linear systems theory [1-5]. These features are especially important in real-time simulation, parameter estimation, and controller design, where rational transfer functions and finite-dimensional state-space models are often preferred. The fractional-order models provide a powerful extension of classical integer-order models. Operators such as the Caputo and Riemann-Liouville derivatives are useful when memory, hereditary behaviour, and diffusion-like effects are essential [6,7]. Such models have been used successfully in viscoelasticity, anomalous diffusion, electrochemical systems, and control applications [8,9]. However, the fractional-order models also introduce additional analytical and computational difficulties. Their nonlocal structure usually leads to history-dependent terms, non-integer powers in the Laplace domain, and non-rational transfer functions. Such features can be valuable for representing memory, but they may complicate real-time implementation and standard control design.

In many applied situations, the objective is not to reproduce true fractional memory. However, one may need a simple and tunable model that moves continuously between known integer-order regimes while preserving locality and rational transfer-function structure [10]. This need appears naturally in control-oriented modelling, where one often balances accuracy, interpretability, and computational efficiency. Classical resistor-capacitor models for instance are attractive for battery management systems because they are simple and suitable for embedded implementation, but they may be too rigid to describe intermediate polarization behaviour. Fractional-order equivalent circuit models can improve flexibility, but they often require nonlocal operators or rational approximations before they can be used with standard control tools.

In this paper, we investigate this modelling need by introducing a local polynomial interpolatory operator based on Lagrange interpolation of selected integer-order operators. It is built as a finite linear combination of classical integer-order derivatives, with coefficients depending polynomially on a real interpolation parameter. Therefore, it remains local and finite-dimensional.

Polynomial interpolation is a classical tool in numerical analysis and approximation theory [11-14]. The contribution of this work is not the Lagrange interpolation formula itself, but its systematic use at the operator level to construct rational and tunable dynamical models. This viewpoint is different from interpolation-space theory, where the main goal is to construct intermediate function spaces or study operator domains [15-17]. Here, the goal is to build local parameter-dependent models that preserve compatibility with ordinary differential equations and classical control analysis.

The proposed operator has several useful structural properties. It recovers the selected integer-order derivatives exactly at the interpolation nodes, depends polynomially on the interpolation parameter, and satisfies a basic Sobolev stability estimate on each fixed node set. More importantly for applications, its Laplace-domain symbol is a polynomial in the transform variable. Hence, differential equations involving the proposed operator reduce exactly to finite-order ordinary differential equations, and the resulting transfer functions are rational. This property makes the approach compatible with standard tools from modern control engineering and linear systems theory [18,19].

Since this operator is local and finite-dimensional, it cannot reproduce the long-memory behaviour of genuine fractional derivatives. This is consistent with the known distinction between locality and fractional behaviour [11,20]. Therefore, the present framework should be viewed as a complement to

fractional calculus, not as a replacement for it. It is intended for applications where a rational, local, and tunable bridge between integer-order models is more useful than a nonlocal memory model.

Our main contributions are as follows. First, we formulate a local polynomial interpolatory derivative operator $D_\alpha^{(k)}$ that connects prescribed integer-order operators through a real tuning parameter α, offering a systematic framework for constructing tunable dynamical models. Second, we establish the fundamental structural properties of the operator, including linearity, exact recovery at interpolation nodes, locality, polynomial dependence on α, and uniform Sobolev stability bounds on fixed stencils. Third, we derive its Laplace-domain representation and demonstrate that equations involving $D_\alpha^{(k)}$ reduce to finite-order ordinary differential equations with rational transfer functions, enabling direct compatibility with classical control tools. Finally, we apply the framework to battery equivalent circuit modelling, showing how the interpolation parameter provides a rational tuning mechanism between static, first-order, and higher-order polarization dynamics, with numerical validation on a synthetic pulse-response benchmark. This operator-level interpolation framework is not the Lagrange interpolation formula itself, but rather its systematic use to bridge integer-order models in a tunable and rational manner.

2. Preliminaries and Notation

Let $I \subseteq \mathbb{R}$ be an interval, and let $f: I \to \mathbb{R}$ be sufficiently smooth. For every integer $m \geq 0$, we denote by $D^m f$ the classical derivative of order m, with

$$D^0 f = f.$$

Thus, D^0 is the identity operator, D^1 is the usual first derivative, etc. For $m \geq 1$, we denote by J^m the m-fold repeated integral operator defined by Cauchy's formula

$$(J^m f)(t) = \frac{1}{(m-1)!}\int_0^t (t-s)^{m-1} f(s)\, ds, \tag{1}$$

where,

$$J^0 f = f.$$

The operators D^m and J^m, with $m \in \mathbb{N}_0$, form the building blocks of the interpolatory construction.

Let $\alpha \in \mathbb{R}$. When a moving local stencil is used, we write

$$n = \lfloor \alpha \rfloor.$$

The parameter α is an interpolation parameter.

The simplest interpolation occurs between two neighbouring integer-order operators. If

$$\alpha \in [n, n+1], \qquad \theta = \alpha - n \in [0,1],$$

then the first-degree interpolatory derivative operator is defined by

$$D_\alpha^{(1)} f = (1-\theta) D^n f + \theta D^{n+1} f \tag{2}$$

Similarly, the first-degree interpolatory integral operator is defined by

$$J_\alpha^{(1)} f = (1-\theta) J^n f + \theta J^{n+1} f \tag{3}$$

At nonnegative integer values, these operators recover the corresponding classical operators exactly:

$$D_m^{(1)} = D^m, \qquad J_m^{(1)} = J^m, \qquad m \in \mathbb{N}_0 \tag{4}$$

This exact recovery property is the basic consistency condition of the construction.

For higher-degree interpolation, more than two integer-order operators are used. Fix an interpolation degree $k \geq 1$. On a moving stencil, if $\alpha \in [n, n+1]$, where $n = \lfloor \alpha \rfloor$, we may choose

$$N_k(\alpha) = \{n, n+1, \dots, n+k\} \tag{5}$$

This choice is convenient when the interpolation window is intended to move with α. However, in applications, it is also useful to prescribe a fixed stencil over a chosen parameter interval. For example, one may use

$$N_2 = \{0,1,2\}$$

for $0 \leq \alpha \leq 2$, to connect algebraic, first-order, and second-order regimes. Thus, the stencil may be either moving or fixed, depending on the modelling purpose. In both cases, the stencil is part of the model and must be chosen according to the integer-order regimes that are intended to be connected.

Let

$$N_k = \{n_0, n_1, \dots, n_k\}$$

denote the chosen stencil, either moving or fixed. The associated Lagrange basis polynomials are

$$L_j(\alpha) = \prod_{\substack{i=0 \\ i \neq j}}^{k} \frac{\alpha - n_i}{n_j - n_i}, \qquad j = 0,1, \dots, k \tag{6}$$

They satisfy the cardinal property.

$$L_j(n_i) = \delta_{ij} \tag{7}$$

where δ_{ij} is the Kronecker delta. This property ensures exact recovery of the selected integer-order operators at the interpolation nodes.

The degree-k interpolatory derivative operator associated with the chosen stencil is defined by

$$D_\alpha^{(k)} f = \sum_{j=0}^{k} L_j(\alpha) D^{n_j} f, \qquad N_k = \{n_0, n_1, \dots, n_k\} \tag{8}$$

By construction, $D_\alpha^{(k)}$ is a finite linear combination of classical integer-order derivatives. Hence, it is local and finite-dimensional. At a node $n_i \in N_k$, the cardinal property gives

$$D_{n_i}^{(k)} f = D^{n_i} f \tag{9}$$

Thus, the proposed operator recovers the selected classical derivatives exactly at the stencil nodes.

The corresponding degree-k interpolatory integral operator may be defined in the same way as

$$J_\alpha^{(k)} f = \sum_{j=0}^{k} L_j(\alpha) J^{n_j} f \tag{10}$$

At every node $n_i \in N_k$, it satisfies

$$J_{n_i}^{(k)} f = J^{n_i} f.$$

In the rest of the paper, the main emphasis is placed on $D_\alpha^{(k)}$, because it leads naturally to tunable differential equations and rational transfer functions.

To illustrate our construction, let us take $k = 1$ and $N_1 = \{n, n+1\}$. Then

$$L_0(\alpha) = n + 1 - \alpha, \qquad L_1(\alpha) = \alpha - n,$$

and hence

$$D_\alpha^{(1)} f = (n + 1 - \alpha) D^n f + (\alpha - n) D^{n+1} f. \tag{11}$$

This agrees with (2), since $\theta = \alpha - n$. In particular, for the fixed stencil $N_1 = \{0,1\}$, one obtains

$$D_\alpha^{(1)} f = (1 - \alpha) f + \alpha f', \qquad 0 \le \alpha \le 1.$$

This case interpolates between an algebraic response and a first-order dynamic response.

Note that, for dimensional consistency, suppose the physical time variable is $\tilde{t}$ with dimension $[T]$. Introduce a normalized time $t = \tilde{t}/t_0$ where $t_0 > 0$ is a characteristic time scale. The normalized derivative is $\frac{d}{dt} = t_0 \, d/d\tilde{t}$. If $\tilde{f}\,(\tilde{t}) = f(t)$ then $D^m f(t) = t_0^m \, \widetilde{D}^m \, \tilde{f}\,(\tilde{t})$. The interpolatory operator in physical variables becomes

$$\widetilde{D}_\alpha^{(k)} \, \tilde{f} = \sum_{j=0}^{k} L_j(\alpha) t_0^{n_j} \widetilde{D}^{n_j} \, \tilde{f},$$

so the coefficients carry distinct dimensional factors $t_0^{n_j}$.

For the fixed stencil $N_2 = \{0,1,2\}$, the Lagrange polynomials are

$$L_0(\alpha) = \frac{(\alpha - 1)(\alpha - 2)}{2},$$

$$L_1(\alpha) = -\alpha(\alpha - 2),$$

and

$$L_2(\alpha) = \frac{\alpha(\alpha - 1)}{2}.$$

Hence

$$D_\alpha^{(2)} f = \tfrac{(\alpha-1)(\alpha-2)}{2} f - \alpha(\alpha - 2) f' + \tfrac{\alpha(\alpha-1)}{2} f''. \tag{12}$$

At the interpolation nodes, this gives

$$D_0^{(2)} f = f, \qquad D_1^{(2)} f = f', \qquad D_2^{(2)} f = f''.$$

Thus, the same fixed-stencil family connects algebraic, first-order, and second-order regimes.

The choice of N_k should be made carefully. Different stencils may produce different intermediate operators, even if they recover the same type of integer-order behaviour at selected nodes. This dependence is not a defect. It is similar to stencil dependence in finite difference methods. In applications, stencil choice may encode boundary effects, directional preference, or the desired transition between physical regimes.

3. Fundamental Properties

In this section, we collect the basic properties of the interpolatory operators introduced in Section 2. Since $D_\alpha^{(k)}$ and $J_\alpha^{(k)}$ are finite linear combinations of classical integer-order operators, the elementary structural properties are immediate.

Throughout this section, let $I \subseteq \mathbb{R}$ be an interval, let $k \geq 1$, and let

$$N_k = \{n_0, n_1, \dots, n_k\}$$

be the chosen stencil, either fixed on a prescribed parameter interval or fixed locally on a moving-stencil interval. We assume that f is sufficiently smooth so that all derivatives appearing in $D_\alpha^{(k)} f$ are well defined. We also write

$$n_{\max} = \max N_k.$$

By definition,

$$D_\alpha^{(k)} f = \sum_{j=0}^{k} L_j(\alpha) D^{n_j} f \tag{13}$$

Theorem 1. *For a fixed interpolation degree k and a chosen stencil N_k, the operator $D_\alpha^{(k)}$ satisfies the following properties.*

1. *For each fixed α, the mapping $f \mapsto D_\alpha^{(k)} f$ is linear.*
2. *At every interpolation node $n_i \in N_k$, $D_{n_i}^{(k)} f = D^{n_i} f$.*
3. *The operator is local. More precisely, $D_\alpha^{(k)} f(t)$ depends only on $f(t), Df(t), \dots, D^{n_{\max}} f(t)$ at the same point t.*
4. *For each fixed f, the map $\alpha \mapsto D_\alpha^{(k)} f$ is polynomial in α of degree at most k as long as the stencil N_k is fixed.*
5. *For every fixed α, $D_\alpha^{(k)} \in \operatorname{span}\{D^{n_0}, D^{n_1}, \dots, D^{n_k}\}$.*

Proof. All statements follow directly from the representation of equation (13). Linearity and locality follow from the corresponding properties of the classical derivatives D^{n_j}. At a node n_i, the cardinal property $L_j(n_i) = \delta_{ij}$ gives

$$D_{n_i}^{(k)} f = \sum_{j=0}^{k} L_j(n_i) D^{n_j} f = D^{n_i} f \tag{14}$$

The polynomial dependence on α follows from the polynomial form of $L_j(\alpha)$, and the finite-dimensional span property is immediate from the definition. □

The same reasoning applies to the integral operator $J_\alpha^{(k)}$. In particular, $J_\alpha^{(k)}$ is linear and satisfies

$$J_{n_i}^{(k)} f = J^{n_i} f$$

at the interpolation nodes. Since the rest of the paper focuses on differential models, the remaining estimates are stated for $D_\alpha^{(k)}$.

Proposition 2. *Let $K \subset \mathbb{R}$ be compact, and suppose that the stencil N_k is fixed for $\alpha \in K$. Then there exists a constant $C_k(K) > 0$ such that $\sum_{j=0}^{k} |L_j(\alpha)| \leq C_k(K), \quad \alpha \in K$. The constant $C_k(K)$ depends only on the interpolation degree, the stencil, and the compact parameter interval K, but not on f.*

Proof. Each $L_j(\alpha)$ is a polynomial, and hence continuous on K. Therefore, the function

$$\alpha \mapsto \sum_{j=0}^{k} |L_j(\alpha)|$$

is continuous on K. Since K is compact, this function attains a finite maximum. This maximum may be taken as $C_k(K)$. □

Theorem 3. *Let $1 \leq p \leq \infty$, and let $f \in W^{n_{\max},p}(I)$. Suppose that the stencil N_k is fixed for $\alpha \in K$, where $K \subset \mathbb{R}$ is compact. Then $\| D_\alpha^{(k)} f \|_{L^p(I)} \leq C_k(K) \max_{0 \leq j \leq k} \| D^{n_j} f \|_{L^p(I)}, \quad \alpha \in K$. Consequently, there exists a constant $\tilde{C}_k(K) > 0$ such that $\| D_\alpha^{(k)} f \|_{L^p(I)} \leq \tilde{C}_k(K) \| f \|_{W^{n_{\max},p}(I)}, \quad \alpha \in K$. Thus $D_\alpha^{(k)} : W^{n_{\max},p}(I) \to L^p(I)$ is bounded uniformly for $\alpha \in K$.*

Proof. Using the definition of $D_\alpha^{(k)}$, we obtain

$$\| D_\alpha^{(k)} f \|_{L^p(I)} = \left\| \sum_{j=0}^{k} L_j(\alpha) D^{n_j} f \right\|_{L^p(I)}.$$

By the triangle inequality,

$$\| D_\alpha^{(k)} f \|_{L^p(I)} \leq \sum_{j=0}^{k} |L_j(\alpha)| \, \| D^{n_j} f \|_{L^p(I)}.$$

Applying the coefficient bound gives

$$\| D_\alpha^{(k)} f \|_{L^p(I)} \leq C_k(K) \max_{0 \leq j \leq k} \| D^{n_j} f \|_{L^p(I)}.$$

Since $n_j \leq n_{\max}$ for every j, the last term is bounded by a constant multiple of $\| f \|_{W^{n_{\max},p}(I)}$. This proves the result. □

This stability result shows that the interpolatory derivative does not require derivatives beyond the highest order included in the stencil. It also confirms that no nonlocal term is introduced. The operator remains within the standard Sobolev framework determined by the largest integer-order derivative used in the stencil.

We next clarify the dependence on α when moving stencils are used. On any parameter interval where the stencil is fixed, the map

$$\alpha \mapsto D_\alpha^{(k)} f$$

is polynomial. If the stencil changes at an integer transition point, then the values of the neighbouring polynomial pieces still agree at the common node, because both pieces recover the same classical derivative. However, derivatives with respect to α need not agree there.

Theorem 4. *Assume that a stencil is fixed on each unit interval and that the corresponding interpolatory operator is denoted by* $D_{\alpha}^{(k)}$. *Then, for each sufficiently smooth* f, *the map* $\alpha \mapsto D_{\alpha}^{(k)} f$ *is polynomial on every interval with fixed stencil and continuous at the interpolation nodes. In general, it is not globally* C^1 *with respect to* α, *unless additional matching conditions are imposed on neighbouring stencils.*

Proof. On an interval where the stencil is fixed, the coefficients $L_j(\alpha)$ are polynomials in α. Hence $D_{\alpha}^{(k)} f$ is polynomial in α with values in

$$\text{span}\{D^{n_0} f, D^{n_1} f, \dots, D^{n_k} f\}.$$

At an interpolation node, the adjacent pieces recover the same classical derivative by the cardinal property of the Lagrange basis. Therefore, the map is continuous at the node. However, if the stencil changes, the neighbouring polynomial pieces are generally built from different interpolation data. Their values agree at the common node, but their α-derivatives need not agree. Hence global C^1 regularity is not guaranteed. □

The choice of stencil is part of the model. If $N_k^{(a)}$ and $N_k^{(b)}$ are two admissible stencils with corresponding basis polynomials $L_j^{(a)}(\alpha)$ and $L_j^{(b)}(\alpha)$, then in general

$$D_{\alpha,a}^{(k)} f \neq D_{\alpha,b}^{(k)} f.$$

More explicitly,

$$D_{\alpha,a}^{(k)} f - D_{\alpha,b}^{(k)} f = \sum_{j=0}^{k} L_j^{(a)}(\alpha) D^{n_j^{(a)}} f - \sum_{j=0}^{k} L_j^{(b)}(\alpha) D^{n_j^{(b)}} f \qquad (15)$$

Thus, different stencils may lead to different intermediate dynamics. This dependence is not a defect. It is analogous to stencil dependence in finite difference methods and should be guided by the modelling purpose.

Theorem 5. *Let* $N_k = \{n_0, n_1, \dots, n_k\}$ *be fixed. Suppose that* $\{T_\alpha\}$ *is a family of operators such that* $T_\alpha \in \text{span}\{D^{n_0}, D^{n_1}, \dots, D^{n_k}\}$, *the map* $\alpha \mapsto T_\alpha$ *is polynomial of degree at most* k, *and* $T_{n_j} = D^{n_j}, \quad j = 0,1,\dots,k$. *Then* $T_\alpha = D_{\alpha}^{(k)}$ *for all* α *on the fixed-stencil parameter interval.*

Proof. For each admissible f, the map $\alpha \mapsto T_\alpha f$ is a polynomial of degree at most k that takes the values $D^{n_j} f$ at the nodes n_j. By uniqueness of Lagrange interpolation,

$$T_\alpha f = \sum_{j=0}^{k} L_j(\alpha) D^{n_j} f = D_{\alpha}^{(k)} f.$$

Since this holds for every admissible f, the operators are equal. □

4. Laplace Transform and Reduction to Ordinary Differential Equations

A central advantage of the interpolatory operator $D_{\alpha}^{(k)}$ is its compatibility with the classical Laplace transform. Since $D_{\alpha}^{(k)}$ is a finite linear combination of integer-order derivatives, its Laplace-domain representation contains only integer powers of the transform variable. Hence, equations involving $D_{\alpha}^{(k)}$ lead to polynomial symbols and rational transfer functions. This property is important in control-oriented

modelling, where finite-dimensional ordinary differential equations and rational transfer functions are often preferred.

Let

$$N_k = \{n_0, n_1, \dots, n_k\}$$

be a chosen stencil, either fixed on a prescribed parameter interval or fixed locally on a moving-stencil interval. The degree-k interpolatory derivative is given by equation (13). Throughout this section, we assume that f is of exponential order and has sufficiently many classical derivatives so that all Laplace transforms used below exist.

Definition 6. The polynomial symbol associated with $D_\alpha^{(k)}$ on the stencil N_k is defined by

$$\sigma_\alpha^{(k)}(s) = \sum_{j=0}^{k} L_j(\alpha) s^{n_j} \tag{16}$$

At every interpolation node $n_i \in N_k$, the cardinal property of the Lagrange basis gives

$$\sigma_{n_i}^{(k)}(s) = s^{n_i} \tag{17}$$

Thus, the symbol of the classical derivative D^{n_i} is recovered exactly at the interpolation nodes.

Proposition 7. *Suppose that $D^{n_j} f$ is of exponential order for every $n_j \in N_k$. Then*

$$\mathcal{L}\left\{D_\alpha^{(k)} f\right\}(s) = \sigma_\alpha^{(k)}(s) F(s) - I_\alpha^{(k)}(s), \tag{18}$$

where

$$F(s) = \mathcal{L}\{f\}(s),$$

and

$$I_\alpha^{(k)}(s) = \sum_{j=0}^{k} L_j(\alpha) \sum_{m=0}^{n_j-1} s^{n_j-1-m} f^{(m)}(0). \tag{19}$$

The inner sum is understood to be zero when $n_j = 0$.

Proof. From the definition given by equation (13), applying the Laplace transform gives

$$\mathcal{L}\{D_\alpha^{(k)} f\}(s) = \sum_{j=0}^{k} L_j(\alpha) \mathcal{L}\{D^{n_j} f\}(s).$$

For $n_j \geq 1$, the classical Laplace formula gives

$$\mathcal{L}\{D^{n_j} f\}(s) = s^{n_j} F(s) - \sum_{m=0}^{n_j-1} s^{n_j-1-m} f^{(m)}(0),$$

while for $n_j = 0$, we have

$$\mathcal{L}\{D^0 f\}(s) = F(s).$$

Substitution gives

$$\mathcal{L}\{D_\alpha^{(k)} f\}(s) = \left(\sum_{j=0}^{k} L_j(\alpha) s^{n_j}\right) F(s) - \sum_{j=0}^{k} L_j(\alpha) \sum_{m=0}^{n_j-1} s^{n_j-1-m} f^{(m)}(0).$$

Using the definition of $\sigma_\alpha^{(k)}(s)$ and $I_\alpha^{(k)}(s)$, we obtain (18). □

In control-oriented transfer-function analysis, homogeneous initial conditions are often assumed. If

$$f^{(m)}(0) = 0, \qquad 0 \le m \le n_{\max} - 1, \tag{20}$$

where $n_{\max} = \max N_k$, then

$$I_\alpha^{(k)}(s) = 0,$$

and therefore

$$\mathcal{L}\left\{D_\alpha^{(k)} f\right\}(s) = \sigma_\alpha^{(k)}(s) F(s). \tag{21}$$

Thus, under homogeneous initial conditions, $D_\alpha^{(k)}$ acts as a polynomial multiplier in the Laplace domain.

We now consider the interpolatory differential equation

$$D_\alpha^{(k)} y(t) + a y(t) = u(t), \qquad a \in \mathbb{R}. \tag{22}$$

Substituting the definition of $D_\alpha^{(k)}$, we obtain

$$\sum_{j=0}^{k} L_j(\alpha) D^{n_j} y(t) + a y(t) = u(t). \tag{23}$$

Therefore, for each fixed α, the interpolatory equation is exactly a classical ordinary differential equation of finite order. Its order is at most $n_{\max}$, and it is exactly $n_{\max}$ whenever the coefficient of the highest derivative term does not vanish.

Under homogeneous initial conditions, taking the Laplace transform of equation (22) gives

$$\sigma_\alpha^{(k)}(s) Y(s) + a Y(s) = U(s).$$

Equivalently,

$$\left(\sigma_\alpha^{(k)}(s) + a\right) Y(s) = U(s). \tag{24}$$

Hence the transfer function is

$$H_\alpha(s) = \frac{Y(s)}{U(s)} = \frac{1}{\sigma_\alpha^{(k)}(s) + a}. \tag{25}$$

Since $\sigma_\alpha^{(k)}(s)$ is a polynomial in s, $H_\alpha(s)$ is rational for every fixed α and every fixed interpolation degree k. The parameter α tunes the model while preserving the rational structure used in standard control analysis.

For the fixed stencil

$$N_1 = \{0,1\},$$

we have

$$D_{\alpha}^{(1)}y = (1-\alpha)y + \alpha y',$$

and

$$\sigma_{\alpha}^{(1)}(s) = (1-\alpha) + \alpha s.$$

The model

$$D_{\alpha}^{(1)}y(t) + ay(t) = u(t), \tag{26}$$

has the transfer function

$$H_{\alpha}(s) = \frac{1}{\alpha s+a+1-\alpha}. \tag{27}$$

At $\alpha = 0$, this gives the static gain

$$H_0(s) = \frac{1}{a+1},$$

while at $\alpha = 1$, it gives the classical first-order transfer function

$$H_1(s) = \frac{1}{s+a}.$$

For $0 < \alpha \leq 1$, the pole is

$$s_{\alpha} = -\frac{a+1-\alpha}{\alpha}. \tag{28}$$

Thus, the pole moves continuously along the real axis as α varies.

For the fixed stencil

$$N_2 = \{0,1,2\},$$

the symbol is

$$\sigma_{\alpha}^{(2)}(s) = \frac{(\alpha-1)(\alpha-2)}{2} - \alpha(\alpha-2)s + \frac{\alpha(\alpha-1)}{2}s^2. \tag{29}$$

Therefore,

$$H_{\alpha}(s) = \frac{1}{\frac{\alpha(\alpha-1)}{2}s^2 - \alpha(\alpha-2)s + a + \frac{(\alpha-1)(\alpha-2)}{2}}. \tag{30}$$

At $\alpha = 0,1,2$, this family recovers static, first-order, and second-order models, respectively. For non-integer values of α, the model remains a finite-dimensional rational system.

5. Application to a Control-Oriented Battery Equivalent Circuit Model

In this section, we present a supporting application that illustrates the modelling role of the interpolatory derivative operator. The aim is not to develop a complete electrochemical battery theory, but to show how $D_{\alpha}^{(k)}$ can be used to construct a local, rational, and tunable dynamical model. This example is appropriate because equivalent circuit models are widely used in battery management systems due to their simplicity, interpretability, and suitability for state estimation and real-time implementation [21].

A standard first-order equivalent circuit model represents the terminal voltage by

$$V(t) = V_{\mathrm{oc}}\big(z(t)\big) - R_0 I(t) - V_p(t), \tag{31}$$

where $V(t)$ is the terminal voltage, $V_{\mathrm{oc}}(z(t))$ is the open-circuit voltage as a function of the state of charge $z(t)$, R_0 is the ohmic resistance, $I(t)$ is the applied current, and $V_p(t)$ is the polarization voltage. The state of charge is commonly modelled by the Coulomb-counting equation [22],

$$\dot{z}(t) = -\frac{\eta}{Q_n} I(t), \tag{32}$$

where Q_n is the nominal capacity and η is the Coulombic efficiency.

In the classical first-order RC polarization model, $V_p(t)$ satisfies

$$\dot{V}_p(t) + \frac{1}{R_p C_p} V_p(t) = \frac{1}{C_p} I(t), \tag{33}$$

where $R_p > 0$ and $C_p > 0$ are the polarization resistance and capacitance. Put

$$a = \frac{1}{R_p C_p}, \qquad b = \frac{1}{C_p}. \tag{34}$$

Then formula (33) becomes

$$\dot{V}_p(t) + a V_p(t) = b I(t). \tag{35}$$

This model is simple and stable, but its transient behaviour is fixed once a and b are chosen.

To introduce a local tuning parameter, we replace the classical derivative in equation (35) by the first-degree interpolatory derivative on the fixed stencil $N_1 = \{0,1\}$:

$$D_\alpha^{(1)} V_p(t) = (1-\alpha) V_p(t) + \alpha \dot{V}_p(t), \qquad 0 \le \alpha \le 1. \tag{36}$$

The proposed interpolatory polarization model is

$$D_\alpha^{(1)} V_p(t) + a V_p(t) = b I(t). \tag{37}$$

Substituting (36) into (37), we obtain

$$(1-\alpha) V_p(t) + \alpha \dot{V}_p(t) + a V_p(t) = b I(t),$$

or

$$\alpha \dot{V}_p(t) + (a + 1 - \alpha) V_p(t) = b I(t). \tag{38}$$

For $0 < \alpha \le 1$, this equation can be written as

$$\dot{V}_p(t) + \lambda_\alpha V_p(t) = \mu_\alpha I(t), \tag{39}$$

where

$$\lambda_\alpha = \frac{a+1-\alpha}{\alpha}, \qquad \mu_\alpha = \frac{b}{\alpha}. \tag{40}$$

Hence the proposed model remains a classical first-order ODE. Its pole and effective time constant are

$$s_\alpha = -\lambda_\alpha = -\frac{a+1-\alpha}{\alpha}, \tag{41}$$

and

$$\tau_\alpha = \frac{1}{\lambda_\alpha} = \frac{\alpha}{a+1-\alpha}. \quad (42)$$

Since $a > 0$ and $0 < \alpha \leq 1$, we have $\lambda_\alpha > 0$, and therefore

$$s_\alpha < 0.$$

Thus, the first-degree interpolatory polarization model is asymptotically stable for all $0 < \alpha \leq 1$.

At $\alpha = 1$, equation (38) becomes the classical first-order RC polarization equation

$$\dot{V}_p(t) + aV_p(t) = bI(t). \quad (43)$$

As $\alpha \to 0^+$, the differential term in (38) becomes negligible and the model approaches the algebraic relation

$$(a+1)V_p(t) = bI(t). \quad (44)$$

Therefore, α provides a continuous local transition between an algebraic polarization law and a first-order dynamic polarization law.

Under homogeneous initial conditions, the Laplace transform of (38) gives

$$(\alpha s + a + 1 - \alpha)V_p(s) = bI(s). \quad (45)$$

That is the transfer function from current to polarization voltage is

$$G_\alpha(s) = \frac{V_p(s)}{I(s)} = \frac{b}{\alpha s + a + 1 - \alpha}. \quad (46)$$

This transfer function is rational for every fixed $0 < \alpha \leq 1$. Consequently, the model remains compatible with standard pole analysis, frequency-domain methods, and real-time control implementation.

The effect of α can be seen explicitly from the pole formula. The classical first-order RC pole is

$$s_1 = -a. \quad (47)$$

The interpolatory pole is

$$s_\alpha = -\frac{a+1-\alpha}{\alpha}.$$

Their difference is

$$s_\alpha - s_1 = -\frac{a+1-\alpha}{\alpha} + a = \frac{(a+1)(\alpha-1)}{\alpha}. \quad (48)$$

For $0 < \alpha \leq 1$, this gives

$$s_\alpha - s_1 \leq 0.$$

For fixed $a > 0$, the interpolatory pole lies to the left of the classical pole when $0 < \alpha < 1$. Hence smaller values of α produce faster polarization transients while preserving stability.

For a constant current pulse

$$I(t) = I_0, \qquad t \geq 0, \quad (49)$$

and initial condition $V_p(0) = V_{p,0}$, equation (39) has the solution

$$V_p(t) = V_{p,0}e^{-\lambda_\alpha t} + \frac{\mu_\alpha I_0}{\lambda_\alpha}\left(1 - e^{-\lambda_\alpha t}\right). \tag{50}$$

Using (40), this becomes

$$V_p(t) = V_{p,0}\ \mathrm{e}^{-\frac{a+1-\alpha}{\alpha}t} + \frac{bI_0}{a+1-\alpha}\left[1 - \mathrm{e}^{-\frac{a+1-\alpha}{\alpha}t}\right]. \tag{51}$$

If $V_p(0) = 0$, then

$$V_p(t) = \frac{bI_0}{a+1-\alpha}\left[1 - \mathrm{e}^{-\frac{a+1-\alpha}{\alpha}t}\right]. \tag{52}$$

Substituting this into (31) gives the terminal voltage response

$$V(t) = V_{\mathrm{oc}}\big(z(t)\big) - R_0 I_0 - \frac{bI_0}{a+1-\alpha}\left[1 - \mathrm{e}^{-\frac{a+1-\alpha}{\alpha}t}\right]. \tag{53}$$

For a short current pulse, $V_{\mathrm{oc}}(z(t))$ may be approximated locally. Since

$$z(t) = z(0) - \frac{\eta I_0}{Q_n}t, \tag{54}$$

we have the first-order approximation

$$V_{\mathrm{oc}}\big(z(t)\big) \approx V_{\mathrm{oc}}\big(z(0)\big) - V'_{\mathrm{oc}}\big(z(0)\big)\frac{\eta I_0}{Q_n}t. \tag{55}$$

Therefore,

$$V(t) \approx V_{\mathrm{oc}}\big(z(0)\big) - V'_{\mathrm{oc}}\big(z(0)\big)\frac{\eta I_0}{Q_n}t - R_0 I_0 - \frac{bI_0}{a+1-\alpha}\left[1 - \mathrm{e}^{-\frac{a+1-\alpha}{\alpha}t}\right]. \tag{56}$$

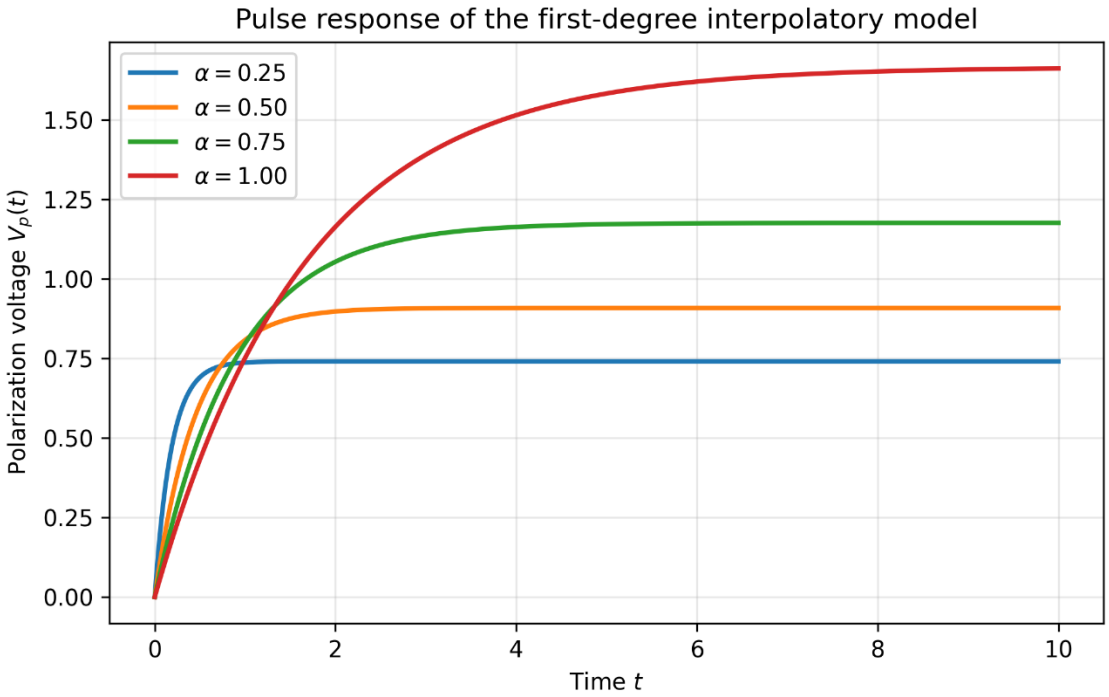

Figure 1 Polarization voltage response $V_p(t)$ under a constant current pulse for several values of the interpolation parameter α. The parameters used for illustration are $a = 0.6$, $b = 1$, $I_0 = 1$, and $V_p(0) = 0$. Smaller values of α produce faster transients, while $\alpha = 1$ recovers the classical first-order RC polarization model.

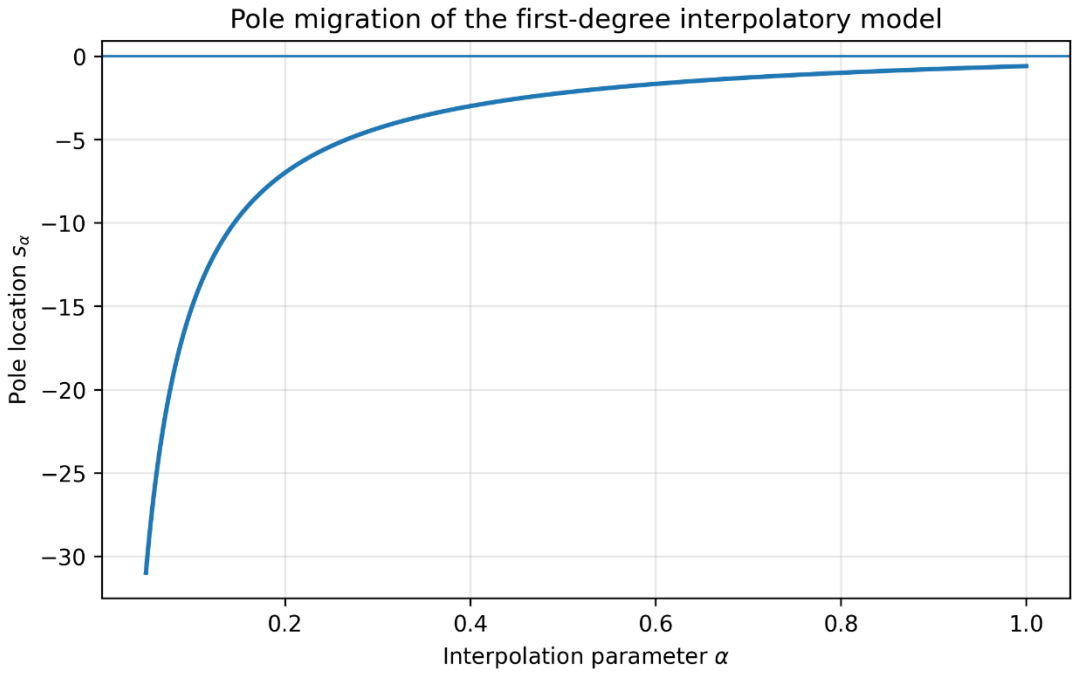

Figure 2 Pole migration of the first-degree interpolatory battery model as the interpolation parameter α varies. For $a = 0.6$, the pole $s_\alpha = -(a + 1 - \alpha)/\alpha$ remains on the negative real axis for $0 < \alpha \leq 1$.

The corresponding pole movement is shown in Figure 2, which provides a control-oriented interpretation of the interpolation parameter. Equation (48) shows explicitly how α modifies the transient rate and the steady polarization level.

To illustrate the effect of α, Figure 1 shows the polarization voltage response under a constant current pulse for several values of α.

It is important to clarify the role of the parameter α. If a, b, and α are all treated as completely free fitting parameters, then the first-degree interpolatory model can be reinterpreted as an ordinary first-order model with reparameterized coefficients. This is in fact not the intended use. In the present application, a and b are regarded as nominal values obtained from a baseline RC model, while α is introduced as an additional low-dimensional tuning parameter. Thus, α provides a structured correction of the nominal model rather than an unrestricted replacement of R_p and C_p. The comparison below is therefore not against a fully refitted first-order RC model, but against a nominal first-order model corrected by one interpolation parameter.

To give a numerical validation of this point, we use a controlled synthetic pulse-response test. This test should be understood as a proof of concept rather than as experimental battery identification. Its purpose is to examine whether the interpolation parameter α can improve a nominal first-order response while preserving a rational finite-order model. We choose a reference signal with two time-scale polarization behaviour:

$$V_{\mathrm{ref}}(t) = 0.70(1 - e^{-3t}) + 0.48(1 - e^{-0.35t}), \qquad 0 \le t \le 10. \tag{57}$$

The reference signal is not generated by the interpolatory model and is not claimed to be experimental battery data. It is used only as a controlled benchmark for testing the effect of the tuning parameter α. We take

$$a = 0.6, \qquad b = 1, \qquad I_0 = 1,$$

and compare the classical first-order model $\alpha = 1$ with the interpolatory model

$$V_\alpha(t) = \frac{1}{a + 1 - \alpha}\left[1 - \mathrm{e}^{-\frac{a+1-\alpha}{\alpha}t}\right], \qquad 0 < \alpha \le 1. \tag{58}$$

The optimal interpolation parameter is computed from

$$\alpha^* = \arg\min_{0<\alpha\le 1}\left\{\frac{1}{N}\sum_{i=1}^{N}[V_{\mathrm{ref}}(t_i) - V_\alpha(t_i)]^2\right\}. \tag{59}$$

Using $N = 201$ equally spaced points on $[0,10]$, the minimum occurs at

$$\alpha^* \approx 0.699. \tag{60}$$

In Figure 3, we compare the reference response, the classical model $\alpha = 1$, and the optimized interpolatory model.

Table 1: Numerical comparison for the synthetic pulse-response validation.

Model	α	RMSE	$E_{\max}$
Classical first-order RC	1.000	0.4224	0.5031
Interpolatory model	0.500	0.1796	0.2564
Interpolatory model	0.750	0.0761	0.1282
Optimized interpolatory model	0.699	0.0521	0.1072

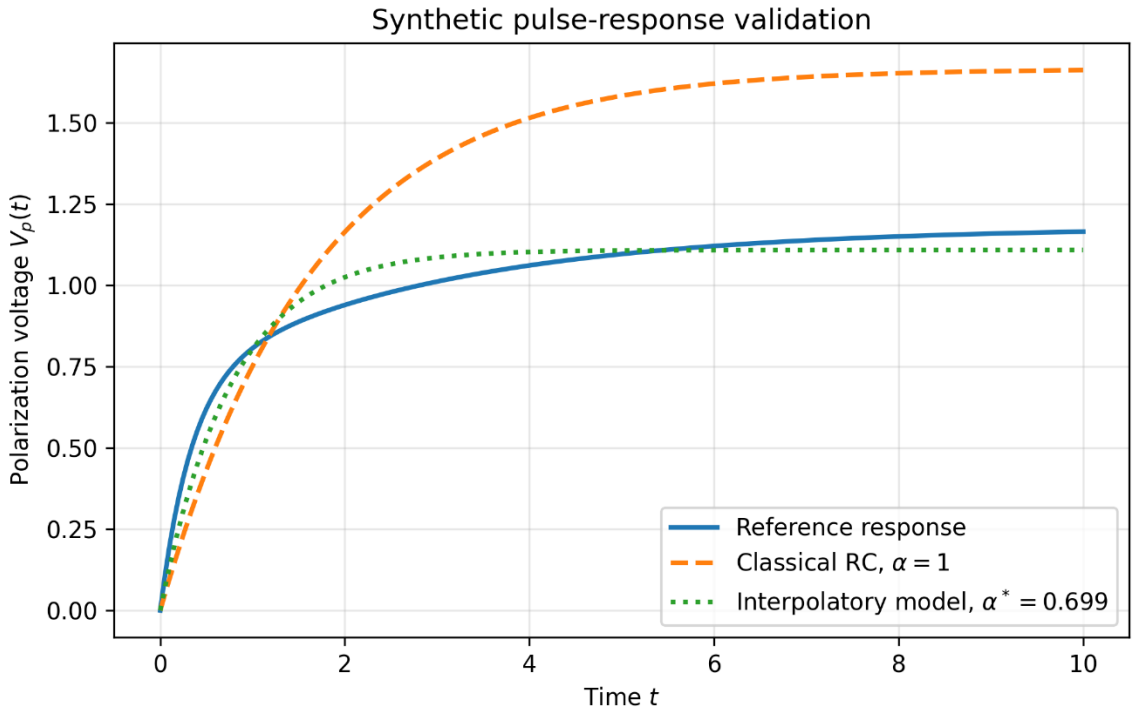

Figure 3 Synthetic pulse-response validation. The reference response is a two-time-scale polarization signal, while the interpolatory model uses the same nominal values $a = 0.6$ and $b = 1$, with only α optimized. The optimized value $\alpha^* \approx 0.699$ improves the fit compared with the classical case $\alpha = 1$.

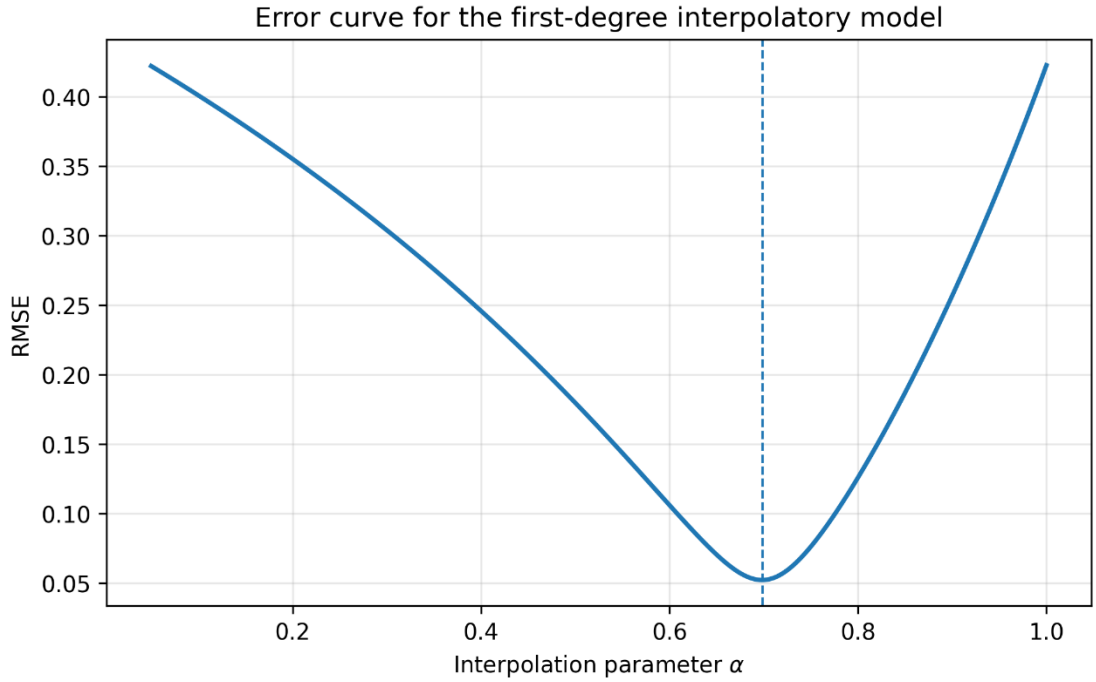

Figure 4 RMSE as a function of the interpolation parameter α for the synthetic validation test. The minimum occurs at $\alpha^* \approx 0.699$, showing that an intermediate local model can fit the reference response better than the fixed classical case $\alpha = 1$.

The corresponding error curve is shown in Figure 4, and the minimum at a non-integer value of α indicates that the interpolation parameter has a visible modelling effect in this controlled test.

The quantitative comparison is given in Table 1. The interpolatory model with $\alpha^* \approx 0.699$ gives a substantially smaller error than the classical first-order model $\alpha = 1$ under the same nominal values of a and b.

This comparison is intended to measure the effect of the single interpolation parameter α, not to replace full parameter identification of a battery model.

The error measures used in Table 1 are

$$\mathrm{RMSE} = \sqrt{\frac{1}{N}\sum_{i=1}^{N}[V_{\mathrm{ref}}(t_i) - V_{\mathrm{model}}(t_i)]^2}, \tag{61}$$

and

$$E_{\max} = \max_{1\le i\le N} |V_{\mathrm{ref}}(t_i) - V_{\mathrm{model}}(t_i)|. \tag{62}$$

This numerical test is not intended to replace experimental battery validation, but it shows that, even with fixed nominal coefficients, the interpolation parameter can provide a useful structured correction while preserving a rational first-order model.

A second-degree model may be used when the aim is to connect algebraic, first-order, and second-order regimes. When stencil $N_2 = \{0,1,2\}$, for instance, we have

$$D_\alpha^{(2)} V_p = \frac{(\alpha-1)(\alpha-2)}{2} V_p - \alpha(\alpha-2)\dot{V}_p + \frac{\alpha(\alpha-1)}{2}\ddot{V}_p. \tag{63}$$

The second-degree interpolatory polarization equation is

$$D_\alpha^{(2)} V_p(t) + aV_p(t) = bI(t). \tag{64}$$

Substitution gives

$$\frac{\alpha(\alpha-1)}{2}\ddot{V}_p(t) - \alpha(\alpha-2)\dot{V}_p(t) + \left[a + \frac{(\alpha-1)(\alpha-2)}{2}\right] V_p(t) = bI(t). \tag{65}$$

Let

$$A_2(\alpha) = \frac{\alpha(\alpha-1)}{2}, \qquad A_1(\alpha) = -\alpha(\alpha-2), \tag{66}$$

and

$$A_0(\alpha) = a + \frac{(\alpha-1)(\alpha-2)}{2}. \tag{67}$$

Then (65) becomes

$$A_2(\alpha)\ddot{V}_p(t) + A_1(\alpha)\dot{V}_p(t) + A_0(\alpha)V_p(t) = bI(t). \tag{68}$$

Under homogeneous initial conditions, the transfer function is

$$G_\alpha(s) = \frac{V_p(s)}{I(s)} = \frac{b}{A_2(\alpha)s^2 + A_1(\alpha)s + A_0(\alpha)}. \tag{69}$$

At $\alpha = 0$, the model reduces to

$$(a+1)V_p(t) = bI(t). \tag{70}$$

At $\alpha = 1$, it reduces to

$$\dot{V}_p(t) + aV_p(t) = bI(t). \tag{71}$$

At $\alpha = 2$, it reduces formally to

$$\ddot{V}_p(t) + aV_p(t) = bI(t). \tag{72}$$

The case $\alpha = 2$ should be interpreted only as a formal endpoint of the polynomial path. It is not necessarily a physically suitable battery polarization model, because it may represent an undamped second-order response. Therefore, in battery applications, the admissible values of α should be restricted by stability and physical consistency.

For the second-degree model to be asymptotically stable, the polynomial

$$A_2(\alpha)s^2 + A_1(\alpha)s + A_0(\alpha)$$

must be Hurwitz. For a second-order polynomial with real coefficients, this is equivalent to

$$A_2(\alpha) > 0, \qquad A_1(\alpha) > 0, \qquad A_0(\alpha) > 0. \tag{73}$$

For $1 < \alpha < 2$, we have

$$A_2(\alpha) > 0, \qquad A_1(\alpha) = \alpha(2-\alpha) > 0.$$

Moreover,

$$A_0(\alpha) = a + \frac{(\alpha-1)(\alpha-2)}{2}.$$

On $1 < \alpha < 2$, the minimum of

$$\frac{(\alpha-1)(\alpha-2)}{2}$$

occurs at $\alpha = 3/2$, and its value is

$$-\frac{1}{8}.$$

Therefore,

$$A_0(\alpha) \geq a - \frac{1}{8}.$$

Hence, if

$$a > \frac{1}{8}, \tag{74}$$

then $A_0(\alpha) > 0$ for all $1 < \alpha < 2$, and the second-degree interpolatory model is asymptotically stable on this interval.

The corresponding characteristic roots are determined by the quadratic polynomial.

$$A_2(\alpha)s^2 + A_1(\alpha)s + A_0(\alpha).$$

Therefore, the second-degree interpolatory model remains a finite-dimensional rational system. Depending on the discriminant, the poles may be real or complex conjugate, but stability is preserved whenever the Hurwitz conditions (73) are satisfied. For the present battery application, this second-degree construction should be viewed as a possible extension rather than as the main validation case. The numerical comparison above focuses on the first-degree model because it already demonstrates the role of α as a structured tuning parameter while keeping the model first order.

The proposed interpolatory model should not be viewed as a replacement for fractional-order equivalent circuit models when long-memory electrochemical effects are essential.

6. Conclusions

This work investigated a local polynomial interpolatory operator for constructing tunable dynamical models between selected integer-order regimes. For a fixed interpolation degree k, the operator $D_\alpha^{(k)}$ is defined as a finite linear combination of classical integer-order derivatives with Lagrange coefficients depending on the interpolation parameter α. The parameter α is not interpreted as a fractional order. However, it is used as a local tuning parameter between prescribed integer-order operators. The operator framework relies on the normalization of physical variables; for non-normalized applications, explicit dimensional scaling factors must be introduced to combine different derivative orders.

The proposed construction recovers the classical derivatives exactly at the interpolation nodes, remains local and finite-dimensional, and satisfies basic stability estimates on fixed stencils. Since the symbol $\sigma_\alpha^{(k)}(s)$ is a polynomial in s, equations involving $D_\alpha^{(k)}$ reduce to finite-order ordinary differential equations and lead to rational transfer functions. This makes the approach compatible with standard tools from ordinary differential equations, transfer-function analysis, and control-oriented modelling. However, several limitations should be emphasized. The operator $D_\alpha^{(k)}$ does not reproduce hereditary memory effects and should not be presented as a fractional derivative. The interpolation degree and stencil are part of the model, and different choices may produce different intermediate dynamics. Moreover, the parameter α should be constrained by stability, physical consistency, and data-fitting requirements. This makes the proposed framework best viewed as a local rational modelling tool for applications where tunability, interpretability, and computational simplicity are more important than exact long-memory representation.

REFERENCES

[1] J. C. Robinson, *An Introduction to Functional Analysis*. Cambridge, U.K.: Cambridge University Press, 2020.
[2] R. Magnus, *Essential Ordinary Differential Equations*. Cham, Switzerland: Springer, 2023.
[3] R. A. Adams and J. J. F. Fournier, *Sobolev Spaces*, vol. 140. Amsterdam, The Netherlands: Elsevier, 2003.
[4] T. Kato, *Perturbation Theory for Linear Operators*. Berlin, Germany: Springer, 1966.
[5] J. Banasiak, A. Bobrowski, M. Lachowicz, and Y. Tomilov, "Semigroups of Operators, Theory and Applications," in *Springer Proceedings in Mathematics & Statistics*. Cham, Switzerland: Springer, 2018.
[6] X.-J. Yang, *General Fractional Derivatives: Theory, Methods and Applications*. Boca Raton, FL, USA: Chapman and Hall/CRC, 2019.
[7] D. Baleanu, *Fractional Calculus: Models and Numerical Methods*, vol. 3. Singapore: World Scientific, 2012.
[8] R. L. Bagley and P. J. Torvik, "A Theoretical Basis for the Application of Fractional Calculus to Viscoelasticity," *J. Rheol.*, vol. 27, no. 3, pp. 201-210, 1983.
[9] C. A. Monje, Y. Chen, B. M. Vinagre, D. Xue, and V. Feliu, *Fractional-Order Systems and Controls: Fundamentals and Applications*. London, U.K.: Springer, 2010.
[10] H. Daoub and F. A. M. Bribesh, “Hermite Interpolatory Operator Framework for Stability-Constrained

Transitions Between Integer-Order Dynamical Systems", *LIJNS*, vol. 2, no. 2, pp. 01-11, Jul. 2026.
[11] J. Shen, T. Tang, and L.-L. Wang, *Spectral Methods: Algorithms, Analysis and Applications*, vol. 41. Berlin, Germany: Springer, 2011.
[12] V. E. Tarasov, "No Nonlocality. No Fractional Derivative," *Commun. Nonlinear Sci. Numer. Simul.*, vol. 62, pp. 157-163, 2018.
[13] W. Gautschi, *Numerical Analysis*, 2nd ed. Basel, Switzerland: Birkhäuser, 2012.
[14] R. A. DeVore and G. G. Lorentz, *Constructive Approximation*, vol. 303. Berlin, Germany: Springer, 1993.
[15] J. Bergh and J. Löfström, *Interpolation Spaces: An Introduction*. Berlin, Germany: Springer, 2012.
[16] J.-L. Lions and J. Peetre, "Sur une classe d'espaces d'interpolation," *Publications Mathématiques de l'IHÉS*, vol. 19, pp. 5-68, 1964.
[17] H. Triebel, *Interpolation Theory, Function Spaces, Differential Operators*. Leipzig, Germany: J. A. Barth, 1995.
[18] K. Ogata, *Modern Control Engineering*. Upper Saddle River, NJ, USA: Prentice Hall, 2010.
[19] T. Kailath, *Linear Systems*. Englewood Cliffs, NJ, USA: Prentice-Hall, 1980.
[20] M. D. Ortigueira and J. A. T. Machado, "What Is a Fractional Derivative?" *J. Comput. Phys.*, vol. 293, pp. 4-13, 2015.
[21] H. He, R. Xiong, and J. Fan, "Evaluation of lithium-ion battery equivalent circuit models for state of charge estimation by an experimental approach," *Energies*, vol. 4, no. 4, pp. 582-598, 2011.
[22] X. Ma, X. Li, Y. Fan, and R. Xiong, "State of charge estimation of a lithium-ion battery based on adaptive Kalman filter method for an equivalent circuit model," *Applied Sciences*, vol. 9, no. 13, p. 2765, 2019.